A subject-specific biomechanical control model for the prediction of cervical spine muscle forces

Maxim van den Abbeele, Fan Li, Vincent Pomero, Dominique Bonneau, Baptiste Sandoz, Sébastien Laporte, Wafa Skalli

A subject-specific biomechanical control model for the prediction of cervical spine muscle forces

Maxim Van den Abbeele[a,*], Fan Li[a,b,**], Vincent Pomero[a], Dominique Bonneau[a], Baptiste Sandoz[a], Sébastien Laporte[a], Wafa Skalli[a]

[a] Arts et Metiers ParisTech, Institut de Biomecanique Humaine Georges Charpak, 151 bd de l'Hopital, 75013 Paris, France
[b] State Key Laboratory of Advanced Design and Manufacturing for Vehicle Body, Hunan University, Yuelushan, Changsha, Hunan, 410082, PR China

ARTICLE INFO

Keywords:
Cervical spine
Muscle force estimation
Intervertebral joint load estimation
Biomechanics

ABSTRACT

Background: The aim of the present study is to propose a subject-specific biomechanical control model for the estimation of active cervical spine muscle forces.
Methods: The proprioception-based regulation model developed by Pomero et al. (2004) for the lumbar spine was adapted to the cervical spine. The model assumption is that the control strategy drives muscular activation to maintain the spinal joint load below the physiological threshold, thus avoiding excessive intervertebral displacements. Model evaluation was based on the comparison with the results of two reference studies. The effect of the uncertainty on the main model input parameters on the predicted force pattern was assessed. The fea-sibility of building this subject-specific model was illustrated with a case study of one subject.
Findings: The model muscle force predictions, although independent from EMG recordings, were consistent with the available literature, with mean differences of 20%. Spinal loads generally remained below the physiological thresholds. Moreover, the model behavior was found robust against the uncertainty on the muscle orientation, with a maximum coefficient of variation (CV) of 10%.
Interpretation: After full validation, this model should offer a relevant and efficient tool for the biomechanical and clinical study of the cervical spine, which might improve the understanding of cervical spine disorders.

1. Introduction

Cervical spine musculature plays an important role in maintaining head-neck equilibrium and stability and in preventing intervertebral joint lesions (Lecompte et al., n.d.; Panjabi et al., 1998; Rousseau et al., 2008). Indeed, spinal instability is related to excessive intervertebral displacements, which induces pain. To limit these displacements, the nervous system controls the spinal musculature (Panjabi, 1992a, 1992b; Panjabi et al., 1989). Thus, abnormal muscle behavior may be an explanatory factor of the etiology of neck pain and cervical spine disorders (Alpayci et al., 2016; Cheng et al., 2014; Falla et al., 2007; Fernández-de-las-Peñas et al., 2008). Furthermore, the developmental mechanisms of surgical complications are not yet fully understood, particularly adjacent segment disease (ASD) and proximal junctional kyphosis (PJK), which might induce a secondary compensation at the level of the cervical spine. Abnormal spine loading and muscular dysfunction could be an issue. Therefore, quantifying the spinal muscle force distribution and the corresponding intervertebral joint load in different configurations could provide valuable information for a biomechanical and clinical evaluation of the patient (Choi, 2003; Moroney et al., 1988a). However, multiple muscle systems are difficult to model because of the well-known redundancy problem, i.e. for any given configuration a multitude of muscles can be recruited (Bernstein, 1967), and because of the limitations of the available measurement techniques.

Various models have been developed to face this issue, including mechanistic models using rigid cables simulating the muscles (Kettler et al., 2002), optimization models based on the mathematical optimization of a cost function considering muscle stresses or energy expenditure (Chancey et al., 2003; Han et al., 1995; Moroney et al., 1988a; Stokes and Gardner-Morse, 1995) and EMG-assisted optimization models adopting a direct relationship between muscle or joint forces and EMG data (Cholewicki et al., 1995; Lo Martire et al., 2017). The proprioception-based regulation model, originally developed for the lumbar spine, with the assumption on the core control strategy that muscles prevent spinal joint overloading and limit intervertebral

* Corresponding author.
** Correspondence to: F. Li, State Key Laboratory of Advanced Design and Manufacturing for Vehicle Body, Hunan University, Yuelushan, Changsha, Hunan 410082, PR China.
E-mail addresses: maxim.VAN-DEN-ABBEELE@ensam.eu (M. Van den Abbeele), lifandudu@163.com (F. Li).

https://doi.org/10.1016/j.clinbiomech.2017.12.001

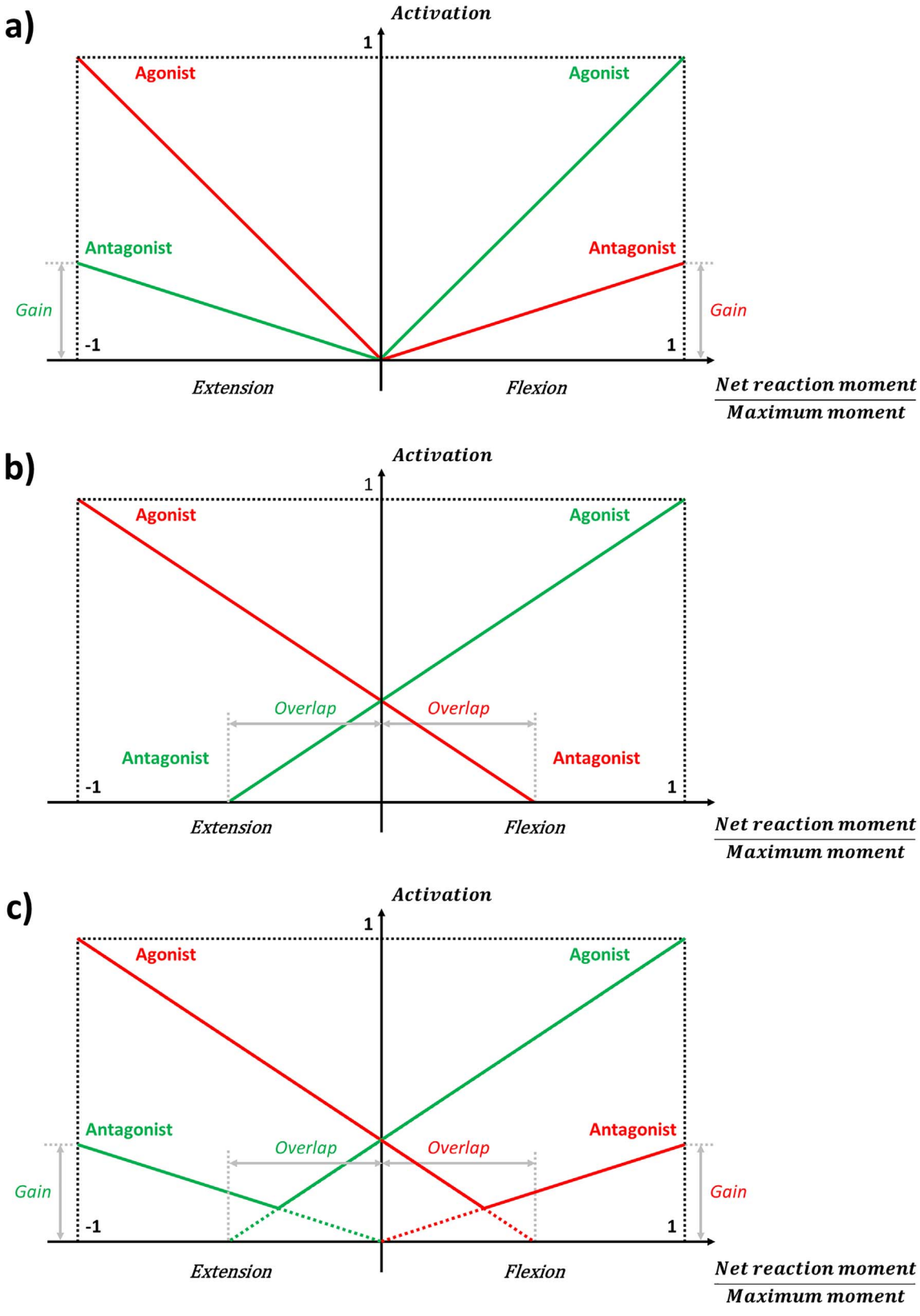

(caption on next page)

displacement to protect spine and spinal cord (Panjabi, 1992a; Panjabi et al., 1989), yields physiologically and mechanically consistent results, independently from EMG measurements. This promotes building such a model from clinical image data (Pomero et al., 2004).

The aim of the present study was to propose a subject-specific proprioception-based biomechanical control model to estimate the cervical spine muscle forces. The results reported in two reference studies were used to evaluate the consistency of the model predictions. In order to progress towards the use of this model in a clinical context, the robustness of the model against the uncertainty on the main model

Fig. 1. Three different interpretations of the agonist and antagonist activation as function of the input command, i.e. the ratio between the net reaction moment and the maximum moment for flexion (0 to 1) and extension (0 to -1), as adapted from Zhou et al. (1996).
In configuration a, the antagonist vs. agonist behavior can be described by a single parameter 'gain', representing the ratio between the antagonist and agonist activation. In configuration b, the parameter 'overlap' determines the antagonist vs. agonist behavior. 'Overlap' represents the percentage of the net reaction to maximum moment ratio at which the agonist and antagonist muscle are both active. In flexion, for instance, the antagonist muscle stays active up to 'overlap', where it reaches zero activity. In full flexion, the only active muscle is the agonist. Configuration c is essentially a combination of configurations a and b. The agonist and antagonist muscles are both active in full flexion (or full extension). The ratio of their activities is given by 'gain'. Because of the 'overlap', the activity of the antagonist muscle never reaches zero, even at low agonist input commands. This configuration was chosen for this study.
The two other parameters 'S' and 'G^{coact}' are used internally in the closed-loop control process and cannot be visually represented. 'S' defines the antagonist sensitivity, i.e. the value above which a muscle is considered antagonist and 'G^{coact}' is a coefficient defining the relative level of agonist-antagonist coactivation.

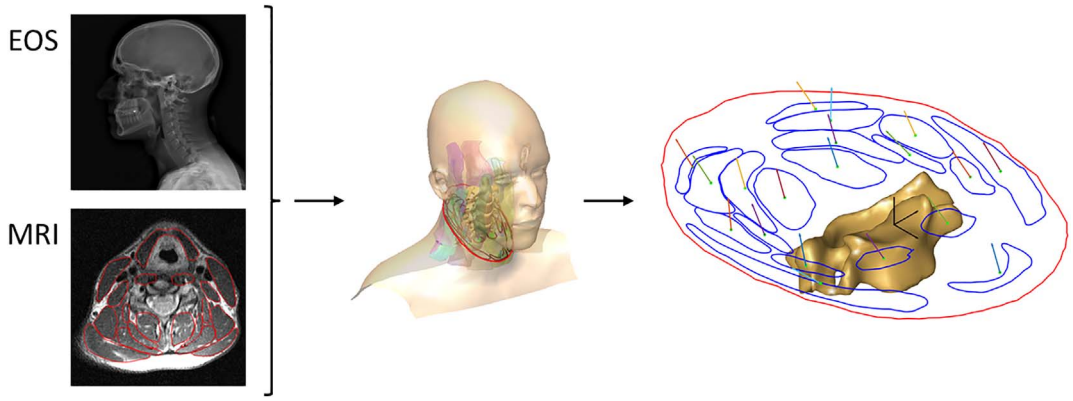

Fig. 2. From the MRI and biplanar X-ray data, a 3D reconstruction of the cervical spine, the external envelope and the muscles can be obtained. This enables the calculation of the geometric parameters of the muscles in the plane of the IVD of interest, here C5-C6.

Table 1
The numerical intervertebral joint forces in each of the four modeled configurations. (PA stands for *postero-anterior*, ML for *medio-lateral* and NA for *not available*).

		PA Shear [N]	ML Shear [N]	Compression [N]	Lateral bending [Nm]	Flexion/extension [Nm]	Torsion [Nm]
Threshold		50	50	1000	3	3	3
Left twist	Current study	62.5	− 29.2	757.1	1.6	1.6	1.6
	Moroney et al. (1988a)	70	33	778	NA	NA	NA
Left bending	Current study	25	− 47.9	759.9	2.2	− 2.2	− 0.9
	Moroney et al. (1988a)	93	125	758	NA	NA	NA
Extension	Current study	196.8	0	1211.4	0	2.9	0
	Moroney et al. (1988a)	135	0	1164	NA	NA	NA
Flexion	Current study	32.2	0	629.4	0	− 2.9	0
	Moroney et al. (1988a)	31	0	558	NA	NA	NA

parameters was quantified and the feasibility of generating this subject-specific model was assessed with a case study based on one subject.

2. Methods

2.1. Model description

2.1.1. The proprioception-based muscle regulation model

The biomechanical muscle control model for the lumbar spine described earlier (Pomero et al., 2004), was adapted to the cervical spine. The model assumes that the spinal musculature protects the spine and the spinal cord by maintaining the intervertebral joint load below the physiological limit, thus preventing the excessive displacement of a vertebra with respect to the subjacent one (Panjabi, 1992a; Panjabi et al., 1989).

The most important model features are detailed hereafter. Let the six-component **wrench** (generalized forces and moments, e.g. (Dumas et al., 2004)) JL represent the intra-articular load, i.e. postero-anterior shear, medio-lateral shear, compression, lateral bending moment, flexion moment and torsion moment. The six-component **wrench** TH describes the corresponding physiological joint load thresholds and F_M the resultant load generated by the muscles, which also contains six components. The six-component **wrench** NetFM represents the net reaction load. From the free-body diagram, the following equation describing mechanical equilibrium can be derived:

$$F_M + JL = NetFM \quad (1)$$

In case JL remains below TH, the need for muscular activity is limited and an energetically economical equilibrium is installed. However, when $JL_i/TH_i > 1$ for a given load component i, spinal overloading is imminent. Muscles are to be activated ($F_M \gg 0$) to ensure mechanical equilibrium and to lower the intervertebral load to physiologically acceptable levels.

This activation strategy is defined in a closed-loop control process. At each iteration, a "regulation request", determined by the JL/TH ratio, is evaluated. Based on this regulation request, the excitation and activation levels of the agonist and antagonist muscles are calculated, from which F_M can be derived. JL can then be updated and compared again with TH. The control loop is ended as soon as JL drops below TH or a minimum is reached.

2.1.2. Muscle regulation request function

The regulation request grossly mimics the functioning of the neuromuscular system, i.e. progressively prompting the muscles to act when the intervertebral joint load JL approaches the physiological

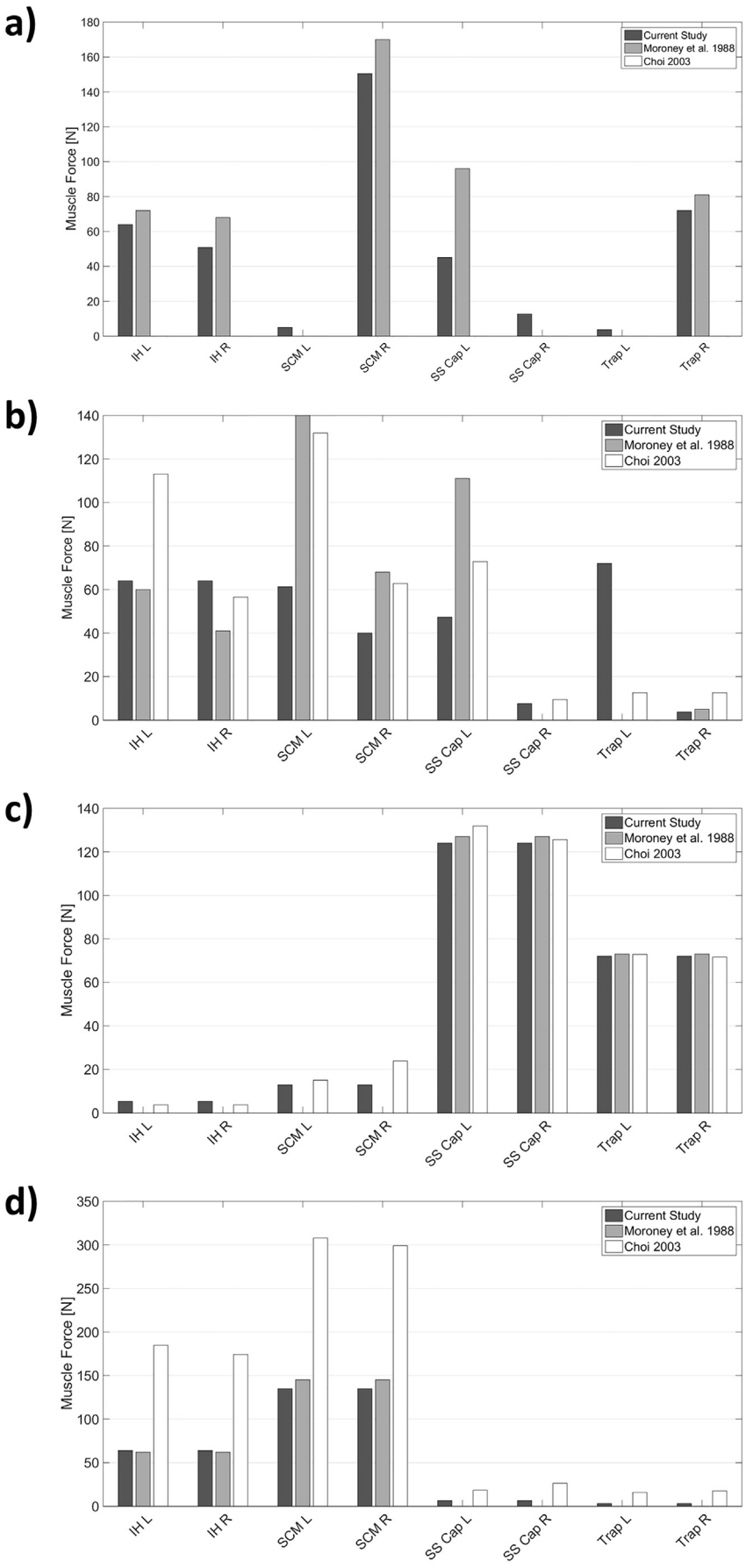

Fig. 3. Comparison of the muscle force predictions with two reference studies for a selection of two anterior and two posterior muscle groups. [L: left; R: right, IH: *infrahyoid*, SCM: *sternocleidomastoideus*, SS cap: *semispinalis capitis*, Trap: *trapezius*].

Table 2
Results of the Monte Carlo analysis allowing the assessment of the model robustness. (PA stands for *postero-anterior* and ML for *medio-lateral*).

	PA Shear [N]	ML Shear [N]	Compression [N]	Lateral bending [Nm]	Flexion/extension [Nm]	Torsion [Nm]
Mean	22.3	− 12.8	− 306.5	0.5	− 0.6	− 0.6
SD	1.3	1.3	9.1	0.04	0.04	0.02
CV	5.6%	− 10%	− 3%	8.9%	− 7%	− 3.1%

Table 3
Results of the correlation analysis of the parameters defining the antagonist law on the C4–C5 joint load.

Spearman correlation Coefficient	S	G^{coact}	Gain	Overlap
Antero-posterior shear	− 0.54	− 0.43	0.13	− 0.36
Medio-lateral shear	− 0.39	0.70	− 0.01	0.53
Compression	0.38	− 0.73	− 0.04	− 0.50
Lateral bending moment	− 0.16	0.78	− 0.01	0.54
Flexion/extension moment	0.50	− 0.69	− 0.04	− 0.47
Axial torsion moment	0.59	− 0.62	− 0.12	− 0.37

limits *TH*. It is represented by a six-component vector Y. For each joint load component i, Y_i is given as follows:

$$Y_i = \alpha \bullet \left(\frac{JL_i}{TH_i}\right)^3 \quad (2)$$

where α is an arbitrarily defined amplification constant.

2.1.3. Agonist muscle activation

MRC_{ij} represents the capacity of the j'th muscle to regulate the i'th joint load component and is determined by the muscle's line of action and moment arm. This 6 by N matrix, with N the number of muscles, is multiplied with Y_i to obtain the excitation level of the agonist muscles. Passing this value through a positive sigmoid function yields the agonist muscle's activation MA_j^{Ag}, with values ranging from 0 (not activated) to 1 (fully activated).

2.1.4. Antagonist muscle activation

For a given external load component, muscle pairs are considered agonist-antagonist when their lines of action are opposed, with a sensitivity S. For each muscle j, the antagonist muscle activation MA_j^{Antag} can then be calculated from the corresponding agonist muscle activation MA_j^{Ag}, considering a certain level of coactivation G^{coact} and a general antagonist law adopted from Zhou et al. (1996), fully determined by two parameters *overlap* and *gain*, (see also Fig. 1c).

2.1.5. Muscle force computation

The agonist and antagonist activations are calculated in parallel and are summed to form the global activation matrix MA. To calculate the individual muscle forces, MA_j is multiplied with the muscle's maximal admissible stress σ_j^{muscle} and its cross sectional surface area CSA_j:

$$F_M = MA \bullet \sigma^{muscle} \bullet CSA \quad (3)$$

By inserting F_M into Eq. (1), JL can be updated.

The above described routine was programmed in Simulink R2014b (The Mathworks Inc., Natick, MA, USA).

2.1.6. Synthesis

This proprioception-based model is able to estimate, independently from EMG recordings, the muscle force distribution and the corresponding joint load at a certain vertebral level. As an input, the following mechanical and geometrical information on the intervertebral joint and the muscles under study are required. For each muscle, the cross sectional surface area, the moment arm with respect to the joint center, the direction vector and the maximal admissible stress are to be obtained. Also, the external load expressed in the local reference frame of the intervertebral joint is a necessary input, as well as the corresponding physiological load threshold.

2.2. Model evaluation

To evaluate the model consistency, the predictions were compared with the results described in Moroney et al. (1988a) and Choi (2003). Moroney et al. (1988a) choose an optimization strategy to estimate the muscle activation pattern and correlated their results with in-vivo EMG data. Choi (2003) used an EMG-based hybrid model (Choi, 2003). The estimated muscle forces were compared in left twist, left bending, extension and flexion with the same input parameters as used in these studies.

2.3. Model robustness and sensitivity study

To progress towards a subject-specific model, built from medical image data, the propagation of the uncertainty on the model input data through the model was quantified.

The muscle's geometrical characteristics, its centroid location, its line of action and its CSA, are obtained from MRI and biplanar X-ray data. With few available slices, the calculation of the muscle's line of action might be inaccurate. In a Monte Carlo analysis, a random error of maximally ± 7.5° was added to the direction cosines, the propagation of which was monitored throughout 1500 simulations.

The influence of the antagonist law parameters (S, G^{coact}, *gain* and *overlap*) and the physiological intra-articular load thresholds (TH), on the muscle force estimation was assessed in a correlation analysis and a full factorial study.

Random pseudo-normal distributions were defined for the antagonism sensitivity S (ranging from 0 to 0.3), the antagonist coactivation G^{coact} (with values between 0 and 0.4), the co-contraction *gain* (limited between 0 and 0.4) and the *overlap* (in the range of 0 and 1). In each of the 2000 simulations, each parameter was randomly sampled from their respective populations.

In accordance with the literature, the joint load threshold values TH_i for postero-anterior shear, medio-lateral shear, compression, flexion/extension moment, lateral bending moment and axial rotation moment were set respectively to 50 N, 50 N, 1000 N, 3 Nm, 3 Nm and 3 Nm (Moroney et al., 1988b; Panjabi et al., 1986; Voo et al., 1998; Yoganandan et al., 2001). To assess the effect of the load threshold values on the model outcome, six series of 20 simulations were performed with six different values for the compressive load threshold, i.e. 200 N, 500 N, 1000 N, 1500 N, 2000 N and 2500 N. In each series, the threshold values for the other five load components were varied from 10% to 200% of their initial values.

The geometrical data and the data regarding the external load were obtained from Moroney et al. (1988a). A resisted left twist was modeled with a focus on the C4/C5 intervertebral joint.

2.4. Model feasibility: a case study

The feasibility of building the subject-specific model is assessed with a case study based on MRI and biplanar X-ray data of one asymptomatic patient (male, 26 years, 65 kg, 1.77 m, BMI 20.8).

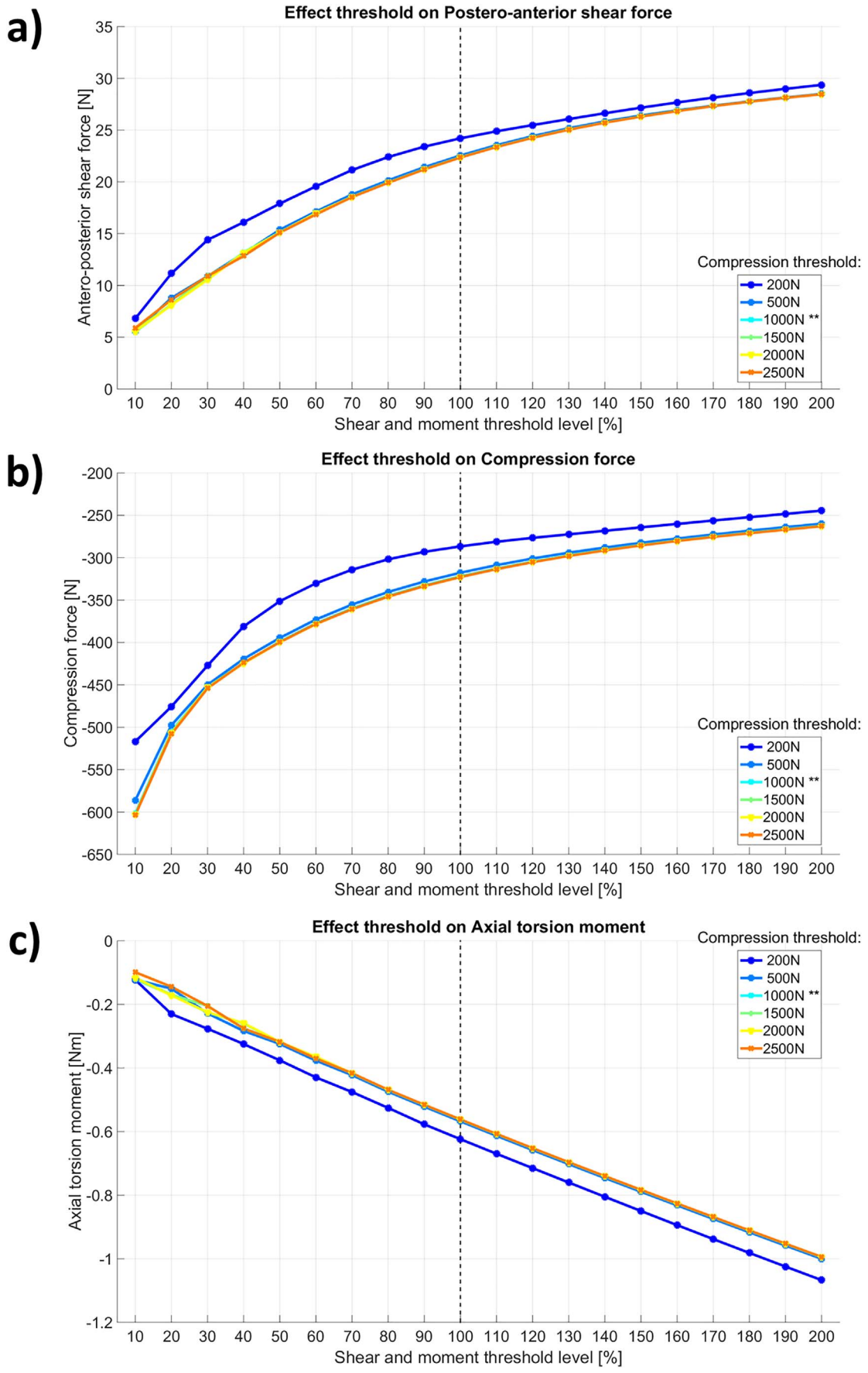

Fig. 4. Effect of the intra-articular load threshold values on the model prediction for the joint force, as obtained with a full-factorial analysis. The graphs present the results of six series of 20 simulations. In each series, the compression threshold remained constant, while the threshold values of the other load components were varied between 10% and 200% of their initial value. The dotted vertical line, as well as the legend entry marked with '**' refer to the reference threshold values.

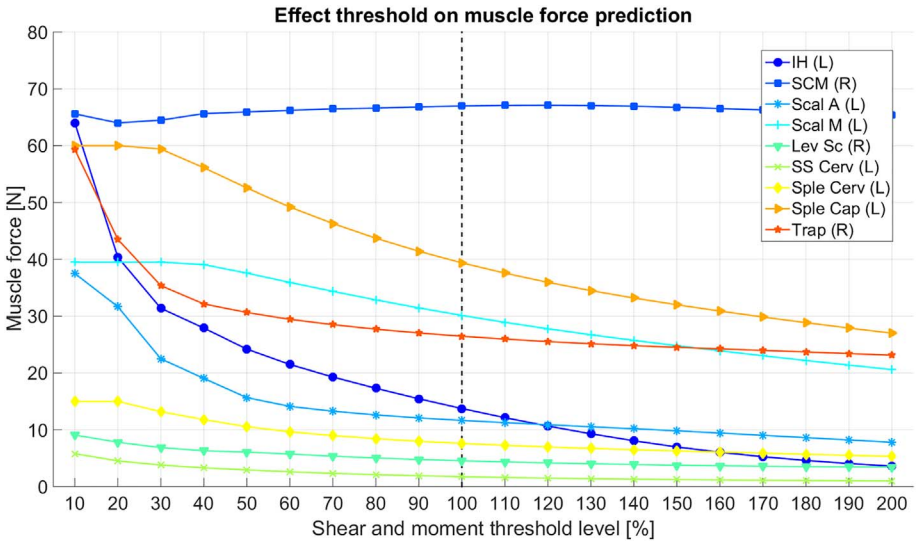

Fig. 5. Effect of the intra-articular load threshold values on the muscle force prediction, as obtained with a full-factorial analysis. The graphs present the results of the 20 simulations performed with a given compression threshold of 1000 N for a selection of ten muscles. The dotted vertical line refers to the reference threshold values. [L: left; R: right, IH: *infrahyoid*, SCM: *sternocleidomastoideus*, Scal A: *scalenus anterioris*, Scal M: *scalenus medius*, Lev Sc: *levator scapulae*, SS Cerv: *semispinalis cervicis*, Sple Cerv: *splenius cervicis*, Sple cap: *splenius capitis*, Trap: *trapezius*].

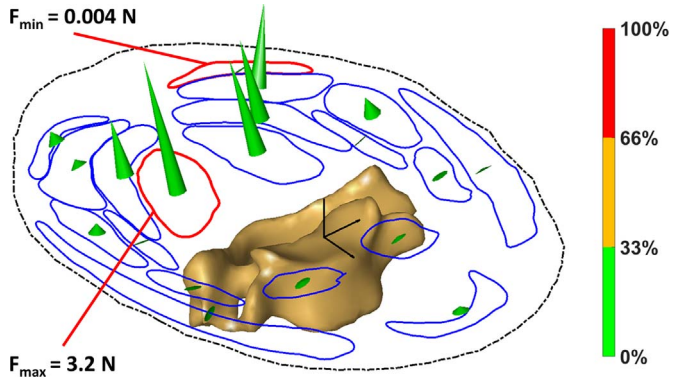

Fig. 6. The predicted muscle force distribution for the erect configuration. The length of the force vectors is proportional to the force magnitude. The color gives an indication of the ratio between the force exerted by the muscle and the force at maximal contraction.

The MRI data was recorded with a 1.5T Philips Achieva MRI system (Philips Medical Systems, Koninklijke Philips N.V, Amsterdam, The Netherlands) with the patient lying down in the *head first – supine* (HFS) position. Biplanar sagittal and frontal X-rays were taken with an EOS-system (EOS imaging SA., Paris, France) with the patient standing upright.

The 3D geometry of 19 cervical spine muscles was reconstructed semi-automatically from the MRI data (Jolivet et al., 2008; Li et al., 2014). The muscle geometry was transferred from the lying to the erect posture via the Kriging method (Trochu, 1993), as described earlier for the lower limb (Hausselle et al., 2012). The muscle CSA's, lever arms and direction cosines were calculated at the level of the C5/C6 intervertebral disc (IVD) plane. The process is visually represented in Fig. 2.

The erect posture was modeled considering the mass of the head and the neck segment superior to the C5/C6 IVD plane. These body segment masses were calculated using barycentremetry based on subject-specific volume data and generic density data (Dempster, 1955). The resultant load was expressed in the reference frame of the C5/C6 IVD plane.

3. Results

For the 3625 simulations performed during this study, the model always fully converged towards a solution, which was obtained in less than 5 s on a regular desktop computer (3.4 GHz i5 CPU and 4Gb RAM).

3.1. Model evaluation

The numerical intervertebral joint load in relation to the physiologically acceptable threshold values and the results published in Moroney et al. (1988a) are listed in Table 1, for each of the four evaluated configurations (left twist, left bending, flexion and extension). The predicted joint loads remained below the threshold values, except for the postero-anterior shear component in left twist and the postero-anterior shear as well as compression components in extension. The joint force amplitudes presented in this study were generally lower than or equal to the values reported by Moroney et al. (1988a), with differences ranging from −70% to 0%. The model predicted higher force amplitudes in extension and to a lesser extent flexion.

The predicted muscle forces for each of the four configurations in relation to those reported by Moroney et al. (1988a) and Choi (2003) are shown in Fig. 3.

Globally, the muscle forces predicted by the current model were lower than or equal to the muscle forces obtained by these authors.

Relative comparison with the results reported by Moroney et al. (1988a) shows that the differences do not exceed 15%, except for five out of the 28 considered muscles in the left twisted configuration (i.e. the right *infrahyoid*, the left and right *levator scapulae* muscles and both *semispinalis* muscles) and for seven muscles in the left inclined configuration (i.e. the right *infrahyoid*, both *sternocleidomastoideus* muscles, the two *semispinalis capitis* muscles and the left and right *trapezius* muscles).

The muscle activation pattern reported in this study agreed with the one Choi (2003) obtained with an EMG-based hybrid model. Moreover, the predicted force amplitudes were lower in left bending and flexion and similar in extension.

3.2. Robustness study

The mean value and the standard deviation for each intervertebral load component, predicted by the model in the 1500 simulations considering a random error on the muscle's direction cosines, are presented in Table 2. The maximum coefficient of variation (CV) was obtained for the medio-lateral shear force (− 10%) and the lateral bending moment (8.9%).

3.3. Sensitivity study

The results of the correlation analysis between the parameters defining the antagonist law and each of the predicted intervertebral load

components are summarized in Table 3. The highest correlation coefficients were found for G^{coact} ($\rho \geq 0.43$), while the lowest were noted for *gain* ($\rho \leq 0.13$).

The effect of varying the intervertebral load threshold values on the predicted postero-anterior shear forces, compression forces and axial torsion moments, i.e. the result of the full factorial analysis, is illustrated in Fig. 4. Adjustment of the compression threshold from 200 N to 500 N impacted all intervertebral joint load components. However, increasing the compression threshold above 500 N did not yield a significant change in joint forces. For example, the postero-anterior shear force decreased from 24.2 N to 22.5 N and from 22.5 N to 22.3 N, with the compression threshold increasing from 200 N to 500 N and from 500 N to 2500 N, respectively. Adjusting the threshold values of the five other load components from 10% to 200% of their initial value, had a more significant effect. For a given compression threshold of 1000 N, the postero-anterior shear force, for instance, increased from its initial value of 22.4 N to 28.5 N when the threshold values were doubled, and decreased to 15.1 N when the threshold values were halved. Doubling the threshold values leads to relatively small changes in muscle forces and force distribution, while halving the threshold values yields a different muscle activation pattern and higher muscle forces, as illustrated in Fig. 5.

3.4. Model feasibility: a case study

The barycentremetric evaluation of the 26 year old male volunteer yielded the following external load, expressed in the IVD reference frame: [26.10 N; −0.15 N; −36.50 N; 0.07 Nm; 0.87 Nm; 0.05 Nm].

The estimated muscle force distribution is visualized in Fig. 6. The corresponding load sensed by the intervertebral joint was 29.80 N of forward shear, 0.15 N of left shear, 47.90 N of compression, 0.04 Nm of right bending, 0.43 Nm of flexion and 0.05 Nm of left axial torsion.

4. Discussion

The aim of the present study was to propose a subject-specific proprioception-based control model for the cervical spine. As such, this study provides an alternative methodology to estimate the active muscle forces for a specific configuration and a specific subject, based on biplanar X-ray and MRI data and independently from EMG-recordings.

Although the importance of the muscular system in ensuring spinal stability and injury prevention has often been confirmed (Falla et al., 2007; Fernández-de-las-Peñas et al., 2008), most studies focused on the lumbar spine. Few authors investigated the behavior of the cervical spine muscular system (Bernhardt et al., 1999; Choi, 2003; Kettler et al., 2002; Moroney et al., 1988a).

To solve the muscle redundancy problem, optimization techniques and EMG-driven methods are generally used (Cholewicki et al., 1995; Han et al., 1995; Moroney et al., 1988a; Stokes and Gardner-Morse, 1995). Validation of these numerical strategies remains an issue, since muscle forces cannot be measured in-vitro or in-vivo. EMG provides a trustworthy indication on the muscle activity of the most superficial muscles, but not necessarily allows the quantification of muscle forces, since the relationship between muscle activity and force should be treated with caution (Hof, 1997, 1984).

The proprioception-based control model changes the paradigm by assuming that the muscular system will act only to protect the spinal joints, i.e. to prevent excessive joint loads and intervertebral displacements, which is naturally a primordial constraint in the cervical spine. This hypothesis on the neuromuscular control, detailed for the first time by Panjabi (1992a, 1992b), could be confirmed experimentally in-vitro (Kettler et al., 2002; Panjabi et al., 1989; Wilke et al., 1995). Its applicability in-vivo could be proven as well, based on EMG-data (Cholewicki and McGill, 1996). Pomero et al. (2004) proposed this control model to predict the muscle force distribution in the lumbar spine. Given the geometrical and functional similarities between the cervical and lumbar spine, the model also applies to the cervical spine, provided that the model parameters are adjusted appropriately.

The comparison with the results obtained with optimization and EMG-assisted optimization techniques, showed that this proprioception-based control model generally predicted lower muscle forces and a lower intervertebral joint load for the cervical spine. One could argue that a more efficient configuration is obtained, which might be preferable from a physiological point of view. The same observation was made by Pomero et al. (2004) for the lumbar spine. This behavior can be explained by the fact that the model distributes the regulation request, defined by the external load and the intervertebral joint load threshold, among the different muscles, based on their direction and cross-sectional surface area instead of using a more theoretical and global optimization technique.

In all four modeled configurations, the predicted muscle forces resembled the estimations reported by Moroney et al. (1988a). For few muscles differences of up to 15% were found. The higher differences noted for, among others, the *sternocleidomastoideus* and the *infrahyoid* muscles can be ascribed to the lack of an explicit consideration of antagonist activation in Moroney's optimization model. Moreover, the predicted activation patterns were very similar to those obtained by Choi (2003) with an EMG-assisted optimization, thus confirming the plausibility of the current model. On the other hand, the results reported by Choi (2003) in the left bended and flexed configuration were clearly higher than those described here. This might be because Choi (2003) used EMG data to provide a first muscle force estimation, which was then further optimized. In the extended configuration, the recorded EMG signals are probably more uniformly distributed among the activated muscles, which is not the case for the other two asymmetrical configurations. The effect of the EMG-related coefficients on the optimization process might thus be less significant.

It should be acknowledged that the current model has its limitations. As in the models described in literature, the influence of the passive elements, i.e. the external envelope, the muscle *fascia* and the ligaments, is not taken into account. This might explain the model behavior in extension, in which the physiological thresholds were not respected. Supplementary work is in progress to include these passive elements in the analysis.

Muscular activity is primordial to maintain the mechanical stability of the spine (Bergmark, 1989; Cholewicki et al., 1995; Panjabi, 1992a). By explicitly modeling, albeit in a simplified manner, the agonist-antagonist interplay, based on Zhou et al. (1996), the concept of mechanical stability was integrated. Furthermore, even in cases where JL remains below TH, certain agonist and antagonist muscles were activated, due to the definition of the antagonist law, which never reaches zero (see also Fig. 1c), and of the regulation request function. However, supplementary constraints might be considered to enable the full integration of mechanical stability.

Although it has been shown that asymmetric configurations are necessary in some cases, a symmetric agonist vs. antagonist behavior was assumed in this study (Zhou et al., 1996). An asymmetric antagonist law might be more adapted when considering mechanical stability.

The third main limitation of this proprioception-based approach is the lack of background data on the model parameters, particularly the physiological load thresholds. Yoganandan et al. (2001) found that cervical intervertebral disc failure occurs under compression forces ranging from 602 N to 910 N. Voo et al. (1998) on the other hand, reported higher compression force limits: mean 1275 N (SD 292 N). Moroney et al. (1988b) found that cervical disc segments failed both in flexion and extension at moments of around 3.40 Nm. To the authors' knowledge, the shear force limits are not yet explored in literature. Only Panjabi et al. (1986) studied the cervical mobility under a maximal shear load of 50 N, but no basis was provided for this value. The threshold values used in this study do not correspond to injury, but rather to a physiological limit, above which muscular regulation is

necessary.

Nevertheless, the sensitivity analysis revealed that the intervertebral joint load threshold markedly affected the model outcome, which is consistent with its functioning, since at each iteration the outcome is weighted against the load threshold value. Decreasing the threshold value decreases postero-anterior shear, but increases compression forces. This means that the muscle activation strategy depends on the status of the intervertebral joint, which might vary in time and from one subject to the other. In situations in which clinical instability was established (i.e. a decreased spinal rigidity) the intervertebral load threshold might be lower. This can induce higher muscle forces, resulting in higher intervertebral compression forces. Furthermore, with poor muscle quality, the situation might be even more acute.

As could be confirmed by the case study, the biggest strength of this proprioception-based control model is its ability to provide physiologically relevant muscle forces and intervertebral joint load, independently from EMG recordings, by combining biplanar X-ray and MRI data. It was also shown that the model behavior was robust to the potential uncertainty on the muscle's direction cosines, calculated from this medical image data. The random error added to the direction cosines did not yield a significantly different intra-articular load or muscle force distribution. After an extensive validation on a representative test population, the proposed model might facilitate the biomechanical and clinical evaluation of the patient.

Acknowledgements

The authors would like to express their gratitude to the ParisTech-BiomecAM chair program on subject-specific modeling, financed by Société Générale, Covea, Proteor and Fondation Cotrel, who supported this study.

Conflict of interest

None.

Appendix A. Supplementary data

Supplementary data to this article can be found online at https://doi.org/10.1016/j.clinbiomech.2017.12.001.

References

Alpayci, M., Şenköy, E., Delen, V., Şah, V., Yazmalar, L., Erden, M., Toprak, M., Kaplan, Ş., 2016. Decreased neck muscle strength in patients with the loss of cervical lordosis. Clin. Biomech. 33, 98–102. http://dx.doi.org/10.1016/j.clinbiomech.2016.02.014.

Bergmark, A., 1989. Stability of the lumbar spine. Acta Orthop. Scand. 60, 1–54. http://dx.doi.org/10.3109/17453678909154177.

Bernhardt, P., Wilke, H.-J., Wenger, K.H., Jungkunz, B., Böhm, A., Claes, L.E., 1999. Multiple muscle force simulation in axial rotation of the cervical spine. Clin. Biomech. 14, 32–44. http://dx.doi.org/10.1016/S0268-0033(98)00031-X.

Bernstein, N.A., 1967. The Coordination and Regulation of Movements. Pergamon Press, Oxford.

Chancey, V.C., Nightingale, R.W., Van Ee, C.A., Knaub, K.E., Myers, B.S., 2003. Improved estimation of human neck tensile tolerance: reducing the range of reported tolerance using anthropometrically correct muscles and optimized physiologic initial conditions. Stapp Car Crash J. 47, 135–153.

Cheng, C.-H., Cheng, H.-Y.K., Chen, C.P.-C., Lin, K.-H., Liu, W.-Y., Wang, S.-F., Hsu, W.-L., Chuang, Y.-F., 2014. Altered co-contraction of cervical muscles in young adults with chronic neck pain during voluntary neck motions. J. Phys. Ther. Sci. 26, 587–590. http://dx.doi.org/10.1589/jpts.26.587.

Choi, H., 2003. Quantitative assessment of co-contraction in cervical musculature. Med. Eng. Phys. 25, 133–140.

Cholewicki, J., McGill, S.M., 1996. Mechanical stability of the in vivo lumbar spine: implications for injury and chronic low back pain. Clin. Biomech. 11, 1–15. http://dx.doi.org/10.1016/0268-0033(95)00035-6.

Cholewicki, J., McGill, S.M., Norman, R.W., 1995. Comparison of muscle forces and joint load from an optimization and EMG assisted lumbar spine model: towards development of a hybrid approach. J. Biomech. 28, 321–331. http://dx.doi.org/10.1016/0021-9290(94)00065-C.

Dempster, W.T., 1955. Space Requirements of the Seated Operator. Wright Air Development Center Air Research and Development Command - Technical Report.

Dumas, R., Aissaoui, R., de Guise, J.A., 2004. A 3D generic inverse dynamic method using wrench notation and quaternion algebra. Comput. Methods Biomech. Biomed. Engin. 7, 159–166. http://dx.doi.org/10.1080/10255840410001727805.

Falla, D., Farina, D., Dahl, M.K., Graven-Nielsen, T., 2007. Muscle pain induces task-dependent changes in cervical agonist/antagonist activity. J. Appl. Physiol. 102, 601–609.

Fernández-de-las-Peñas, C., Falla, D., Arendt-Nielsen, L., Farina, D., 2008. Cervical muscle co-activation in isometric contractions is enhanced in chronic tension-type headache patients. Cephalalgia 28, 744–751. http://dx.doi.org/10.1111/j.1468-2982.2008.01584.x.

Han, J.S., Goel, V.K., Ahn, J.Y., Winterbottom, J., McGowan, D., Weinstein, J., Cook, T., 1995. Loads in the spinal structures during lifting: development of a three-dimensional comprehensive biomechanical model. Eur. Spine J. 4, 153–168.

Hausselle, J., Assi, A.A., El Helou, A., Jolivet, E., Pillet, H., Dion, E., Bonneau, D., Skalli, W., 2012. Subject-specific musculoskeletal model of the lower limb in a lying and standing position. Comput. Methods Biomech. Biomed. Engin. 17, 480–487. http://dx.doi.org/10.1080/10255842.2012.693173.

Hof, A.L., 1984. EMG and muscle force: an introduction. Hum. Mov. Sci. 3, 119–153. http://dx.doi.org/10.1017/CBO9781107415324.004.

Hof, A.L., 1997. The relationship between electromyogram and muscle force. Sportverletz. Sportschaden 11, 79–86. http://dx.doi.org/10.1017/CBO9781107415324.004.

Jolivet, E., Daguet, E., Pomero, V., Bonneau, D., Laredo, J.-D., Skalli, W., 2008. Volumic patient-specific reconstruction of muscular system based on a reduced dataset of medical images. Comput. Methods Biomech. Biomed. Eng. 11, 281–290. http://dx.doi.org/10.1080/10255840801959479.

Kettler, A., Hartwig, E., Schultheiss, M., Claes, L., Wilke, H.-J., 2002. Mechanically simulated muscle forces strongly stabilize intact and injured upper cervical spine specimens. J. Biomech. 35, 339–346. http://dx.doi.org/10.1016/S0021-9290(01)00206-8.

Lecompte, J., Maïsetti, O., Bonneau, D., n.d. Biomécanique du rachis cervical & whiplash. Sauramps Medical.

Li, F., Laville, A., Bonneau, D., Laporte, S., Skalli, W., 2014. Study on cervical muscle volume by means of three-dimensional reconstruction. J. Magn. Reson. Imaging 39, 1411–1416. http://dx.doi.org/10.1002/jmri.24326.

Lo Martire, R., Gladh, K., Westman, A., Äng, B.O., 2017. Neck muscle EMG-force relationship and its reliability during isometric contractions. Sports Med. 3, 16. http://dx.doi.org/10.1186/s40798-017-0083-2.

Moroney, S.P., Schultz, A.B., Miller, J.A.A., 1988a. Analysis and measurement of neck loads. J. Orthop. Res. 6, 713–720. http://dx.doi.org/10.1002/jor.1100060514.

Moroney, S.P., Schultz, A.B., Miller, J.A.A., Andersson, G.B.J., 1988b. Load-displacement properties of lower cervical spine motion segments. J. Biomech. 21, 769–779. http://dx.doi.org/10.1016/0021-9290(88)90285-0.

Panjabi, M.M., 1992a. The stabilizing system of the spine. Part I. Function, dysfunction, adaptation, and enhancement. J. Spinal Disord. Tech. http://dx.doi.org/10.1097/00002517-199212000-00001.

Panjabi, M.M., 1992b. The stabilizing system of the spine. Part II. Neutral zone and instability hypothesis. J. Spinal Disord. 5, 390–396. http://dx.doi.org/10.1097/00002517-199212000-00002.

Panjabi, M.M., Summers, D.J., Pelker, R.R., Videman, T., Friedlaender, G.E., Southwick, W.O., 1986. Three-dimensional load-displacement curves due to forces on the cervical spine. J. Orthop. Res. 4, 152–161. http://dx.doi.org/10.1002/jor.1100040203.

Panjabi, M.M., Abumi, K., Duranceau, J., Oxland, T., 1989. Spinal stability and intersegmental muscle forces. A biomechanical model. Spine (Phila Pa 1976). http://dx.doi.org/10.1097/00007632-198902000-00008.

Panjabi, M.M., Cholewicki, J., Nibu, K., Babatl, L.B., Dvorak, J., 1998. Critical load of the human cervical spine: an in vitro experimental study. Clin. Biomech. 13, 11–17. http://dx.doi.org/10.1016/S0268-0033(97)00057-0.

Pomero, V., Lavaste, F., Imbert, G., Skalli, W., 2004. A proprioception based regulation model to estimate the trunk muscle forces. Comput. Methods Biomech. Biomed. Engin. 7, 331–338. http://dx.doi.org/10.1080/1025584042000327115.

Rousseau, M.-A., Pascal-Moussellard, H., Catonné, Y., Lazennec, J.-Y., 2008. Anatomie et biomécanique du rachis cervical. Rev. Rhum. 75, 707–711. http://dx.doi.org/10.1016/j.rhum.2008.06.001.

Stokes, I.A.F., Gardner-Morse, M., 1995. Lumbar spine maximum efforts and muscle recruitment patterns predicted by a model with multijoint muscles and joints with stiffness. J. Biomech. 28, 173–186. http://dx.doi.org/10.1016/0021-9290(94)E0040-A.

Trochu, F., 1993. A contouring program based on dual kriging interpolation. Eng. Comput. 9, 160–177.

Voo, L.M., Pintar, F.A., Yoganandan, N., Liu, Y.K., 1998. Static and dynamic bending responses of the human cervical spine. J. Biomech. Eng. 120, 693–696.

Wilke, H.-J., Wolf, S., Claes, L.E., Arand, M., Wiesend, A., 1995. Stability increase of the lumbar spine with different muscle groups: a biomechanical in vitro study. Spine (Phila Pa 1976). http://dx.doi.org/10.1097/00007632-199501150-00011.

Yoganandan, N., Kumaresan, S., Pintar, F.A., 2001. Biomechanics of the cervical spine part 2: cervical spine soft tissue responses and biomechanical modeling. Clin. Biomech. 16, 1–27.

Zhou, B.H., Baratta, R.V., Solomonow, M., Olivier, L.J., Nguyen, G.T., D'Ambrosia, R.D., 1996. Evaluation of isometric antagonist coactivation strategies of electrically stimulated muscles. IEEE Trans. Biomed. Eng. 43, 150–160.